Journal on Mechanics of Solids, 1:1 (2022) 39-59
ISSN 2975-8262
DOI: 10.24840/2975-8262_001-001_001818

Received: 26 September, 2022
Accepted: 7 October, 2022
Published: 11 November, 2022

Bi-material Flywheels and Castigliano's Theorems: a Case Study

Paulo M. S. T. de Castro
Emeritus Professor, Universidade do Porto, Faculdade de Engenharia, Rua Dr Roberto Frias, 4200-465 Porto, Portugal. ORCID 0000-0003-3202-1343

Author Keywords
Castigliano's Theorems, Flywheels, Rim and Spokes, Stress Analysis, Energy Storage Systems

Type: Case Study

Open Access
Peer Reviewed

Abstract
The analytical stress analysis of rim and spokes flywheels is revisited in this paper. A brief survey of mechanical energy storage gives a contextualization for the work. Then, the use of Castigliano's theorems for the stress analysis of a rotating rim and spokes flywheel is recalled. The origin of widely available design formulas is elucidated and their rational is discussed. A hitherto unpublished analytical stress analysis for a bi-material flywheel is derived and a parametric solution is presented and discussed.

Notation

A	cross section area
E	Young's modulus
g	acceleration of gravity
I	inertia moment of the cross section
q	weight per unit length of centerline
r	radius of rim centerline
w	load per unit length
y	length
α	half of the angle between consecutive spokes
γ	weight per unit volume
ω	flywheel rotational speed
1	subscript associated with spokes (except where noted)

1. Introduction

This paper is organized as follows: a concise survey of flywheels is presented in the introductory section; in the next section the analytical stress analysis for rotating rim and spokes flywheels is recalled. Then a detailed example is worked out, and finally the analytical solution for the bi-material case is derived and the origin of a practical formula is elucidated. Given their laborious nature, analytical derivations are mainly included in two appendixes.

Historical note and outlook

A flywheel stores rotational kinetic energy. The flywheel accelerates when it accumulates energy and decelerates when delivering its accumulated energy. Rotational kinetic energy is proportional to moment of inertia about the axis of rotation, and this favors rim and spokes compared with compact disc solutions.

Many textbooks present the basic Mechanics of flywheels, see *e.g.* Mata *et al.* (Mata 2016). A treatise on flywheels (one of the few textbooks solely dedicated to these machine elements) is due to Genta (Genta 1985). A presentation of the stress analysis of rotating discs is given *e.g*. by Vullo and Vivio (Vullo and Vivio 2013).

Given the potentially disastrous consequences of their failures, flywheels are among the first machine elements object of detailed analysis, see *e.g.* Kimball and Barr (Kimball and Barr 1909) by Kimball (past ASME president) and Barr, or Kent in ASME Transactions (Kent 1895). Among the pioneers of this field, Pippard's article (Pippard 1924) containing a discussion by Longbottom (Longbottom 1924) should be mentioned.

As technology evolved, flywheels have found - and have lost – applications: recall the steam engine, or presses where flywheels are dismissed as servo presses gain market share, or the internal combustion engine soon to be replaced for the sake of decarbonized mobility. Nevertheless, irrespective of varying specific market opportunities, the need for ever more strict energy management procedures ensures the continued interest in energy storage systems (ESS).

Situations where energy is wasted in useless forms if not recovered for useful application, are a feature of everyday life. Flywheel energy storage systems (FESS) are a possible answer in a variety of sectors, including construction equipment, cranes, space, transportation, grid, etc. Comprehensive literature reviews discuss trends (Liu and Jiang 2007) and list industrial applications, see *e.g.* Hedlund *et al*. focused on automotive applications (Hedlund, Lundin, de-Santiago, Abrahamsson, and Bernhoff 2015), Babuska *et al.* focused on space (Babuska, Beatty, deBlonk, and Fausz 2004), and Amiryar and Pullen focused on grid applications, (Amiryar and Pullen 2017). Flywheels as alternatives to electrochemical batteries have been studied by EPRI for long, *e.g*. (Richma 1997). For energy storage technologies as batteries, flywheels etc., discharging time versus power is a relevant aspect for their characterization, *e.g.* (Akhil 2015), (AL-Shaqsi, Sopian, and Al-Hinai 2020), (Chen, Cong, Yang, Tan, Li, and Ding 2009), (Pärnamäe 2020), another being energy density *vs*. power density, *e.g*. (Luo, Wang, Dooner, and Clarke 2015), (Ibrahim, Ilinca, and Perron 2008).

Examples of current industrial developments involve very high speeds made possible by the use of carbon fibres (Kitade 2000), advanced tribological solutions for bearings, rotation under vacuum and enhanced safety measures against catastrophic failure, *e.g.* Ricardo PLC (RICARDO PLC 2011), Beacon Power (Beacon Power 2018) and others. PUNCH Flybrid KERS (kinetic energy recovery systems) were used *e.g*. in formula 1, (Buchroithner 2019), (PUNCH Flybrid 2022), (Buchroithner 2018). Several current applications are discussed in detail in a special issue of the journal *Energies* (Pullen 2021). Even *The Economist* magazine devoted attention to the subject (The Economist 2011) !

Rim and spoke flywheels

As a result of rotational speed ω rad/s, the circumferential stress in a ring is

$$\sigma_0 = \frac{\gamma}{g}(\omega r)^2 \tag{1}$$

This solution also concerns a rim whose deformation is unaffected by spokes. In this case, the rim does not undergo bending, but only increases the perimeter and therefore the radius; circumferential strain would be

$$\varepsilon = \frac{\sigma_0}{E} = \frac{1}{E}\frac{\gamma}{g}(\omega r)^2 \tag{2}$$

and increase in radius $\Delta r = r\varepsilon$. Conversely, inextensible rays would lead to the existence of bending only, caused by a uniformly distributed load per unit of arc length, of value

$$w = \frac{q}{g}\omega^2 r \tag{3}$$

For this situation, a readily available solution for a beam of length *l* built-in at both ends, subjected to load per unit length w, *e.g.* (Budynas and Nisbett 2011),

$$M = \frac{w}{12}\left(6lx - 6x^2 - l^2\right) \tag{4}$$

being

$$M_{\max} = \frac{w \times l^2}{12} \tag{5}$$

and

$$M_{\min} = \frac{M_{\max}}{2} = \frac{w \times l^2}{24} \tag{6}$$

Now the stress varies along the arc, assuming the highest value for the section corresponding to a spoke, where the bending moment is $M_{\max} = w \times l^2 / 12$ and the local maximum stress is

$$\sigma = \frac{M_{\max} y_{\max}}{I} \tag{7}$$

where *I* is the inertia moment of the rim cross section and $y_{\max}$ the longest distance from the neutral axis, in the cross section.

These two limit cases are described for example, in Collins *et al*. (Collins , Busby, and Staab 2010). Both are approximations that try to avoid the real resolution of the problem, in which the interaction between the ring and the spokes must be modeled, leading to the ring being subject to bending and axial load.

The maximum stress on the rim is the sum of the circumferential stress due to normal effort and bending. The values of one and the other depend, of course, on the increase in length of the spokes; if this is such that the rim deforms freely, then the rim does not bend; if the spokes are inextensible, then the rim will be subject to bending only. For an intermediate spoke extension value, the rim will be in equilibrium partly due to normal effort and partly due to the restrictive action of the spokes. Since the expansion of the rim is directly proportional to the expansion of the spokes, then the rim stress due to normal effort is also proportional to the extension of the rays. If, for example, the spokes suffer 1/3 of the increase in length required for free expansion of the ring, then the bending stress will be proportional to 2/3 of the centrifugal force on the ring.

Pioneering studies by Lanza (Lanza 1895) suggest that the stress state of a flywheel of this type can be roughly estimated as resulting from ¾ of the stress corresponding to the free expansion of the rim, plus ¼ of the stress corresponding to the bending assuming inextensible spokes.

$$\sigma = \left(\frac{3}{4}\right)\frac{\gamma}{g}(\omega r)^2 + \left(\frac{1}{4}\right)\frac{M_{\max} y_{\max}}{I} \tag{8}$$

This traditional approach, *e.g.* Faires (Faires 1980), is still sometimes used, see *e.g*. Khurmi, Gupta (Khurmi and Gupta 2005) and Lingaiah (Lingaiah 2004).

2. Recall of the basic analysis

For those interested in the history of science and technology, it is interesting to know of Castigliano's fight to ensure recognition of authorship of his theorems (Kardestuncer 1978), which are the object of continuing attention, *e.g*. (Dahlberg 2004).

In the many editions of his book 'Strength of Materials', *e.g.* (Timoshenko 1969), Timoshenko presents a solution for stress analysis of flywheel consisting of a rim and spokes based on the use of Castigliano's theorems. In (Timoshenko 1969) the solution is credited to others as Longbottom (Longbottom 1924). Figure 1 shows the notation used, noting that the angle between two consecutive spokes is 2α. The angle φ is counted from the bisector between two rays and assumes values $0 \le \varphi \le \alpha$.

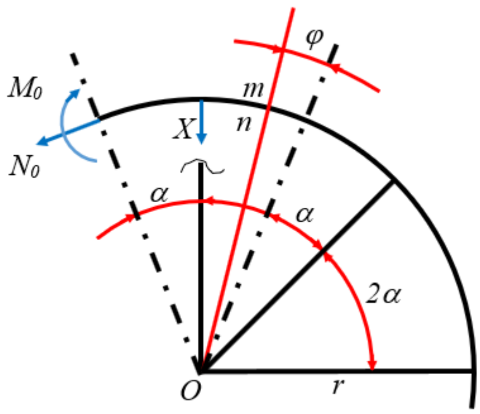

Figure 1. Centerlines of rim and spokes; notation. Dashed black lines represent bisectors between spokes. Full black lines represent spokes.

Remember that the centrifugal force per unit length of rim is $(q/g)\omega^2 r$.

Cross sections of the rim corresponding to bisector locations will be subjected to normal effort N_0 and bending moment M_0, but given symmetry suffer no rotation or shear effort, Figure 1. X being the force that connects the spoke and the ring, the equilibrium of forces in the vertical direction is:

$$2N_0 \sin\alpha + X - \frac{q\omega^2 r}{g} 2r \sin\alpha = 0 \rightarrow N_0 = \frac{q\omega^2 r^2}{g} - \frac{X}{2\sin\alpha} \quad (9)$$

In a generic cross section characterized by the angle φ (section *mn*) counted from a bisector, there will be normal effort N, the calculation of which is facilitated by Figure 2.

$$N = N_0 \cos\varphi + \frac{q\omega^2 r}{g} 2r \left(\sin\left(\frac{\varphi}{2}\right)\right)\left(\sin\left(\frac{\varphi}{2}\right)\right) = \frac{q\omega^2 r^2}{g} - \frac{X\cos\varphi}{2\sin\alpha} \quad (10)$$

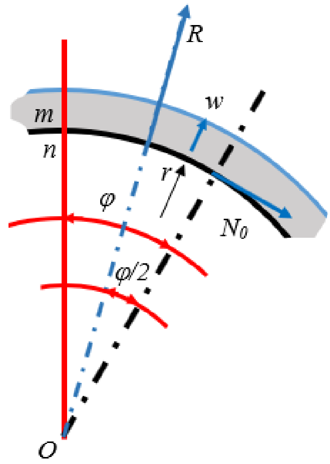

$$R = 2r\sin\left(\frac{\varphi}{2}\right)\times\frac{q}{g}\omega^2 r$$
$$w = \frac{q}{g}\omega^2 r$$

Figure 2. The inertial force per unit length of the rim (w) is schematically represented in grey, and for the angle φ considered its resultant is R. φ is counted from the bisector between spokes.

Figures 3a and 3b help to clarify that in a generic cross section *mn* characterized by the angle φ the bending moment will be

$$M = M_0 - N_0 r\left(1-\cos\varphi\right) + \frac{q\omega^2 r^3}{g}2\sin^2\left(\frac{\varphi}{2}\right) = M_0 + \frac{Xr}{\sin\alpha}\sin^2\left(\frac{\varphi}{2}\right) \quad \textbf{(11)}$$

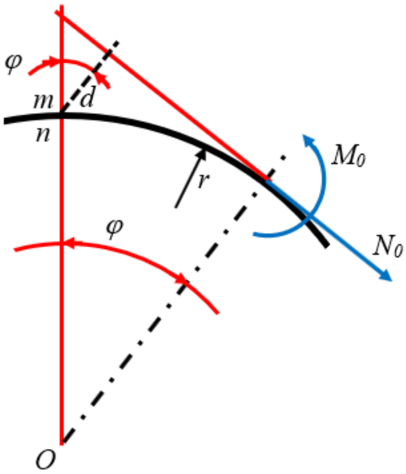

$$\frac{d}{r} = \frac{d/\cos(\varphi)}{r + d/\cos(\varphi)}$$
$$d = r - r\cos(\varphi)$$
$$M = -N_0\left(r - r\cos(\varphi)\right) + M_0 + f(R)$$

a - Calculation of bending moment in section *mn* (φ) due to N_0 .

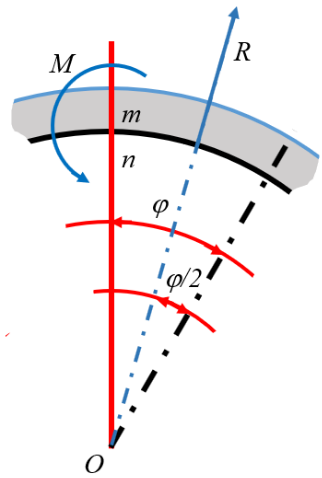

$$M = \frac{q}{g}\omega^2 r\times 2r\sin\left(\frac{\varphi}{2}\right)\times r\sin\left(\frac{\varphi}{2}\right) +$$
$$+ M_0 + f(N_0)$$

b – Calculation of bending moment in section *mn* (φ) due to centrifugal force acting on the rim. M_0 and N_0 exist at the bisector section.

Figure 3. Bending moment in section *mn* characterized by angle φ.

The values of M_0 and of X can be calculated in this indeterminate elastic structure using Castigliano's theorem. For this, it is necessary to calculate the elastic deformation energy in the ring, U_1 , and in the spoke, U_2 . Considering one spoke and the corresponding rim length from -α to +α,

$$U_1 = 2\int_0^\alpha \frac{M^2 r d\varphi}{2EI} + 2\int_0^\alpha \frac{N^2 r d\varphi}{2EA} \quad \textbf{(12)}$$

As for the spoke, it is necessary to calculate the normal effort N_1 for any distance ρ to the center of the flywheel, see Figure 4, resulting:

$$N_1 = X + \frac{q_1 \omega^2}{2g}\left(r^2 - \rho^2\right) \quad \textbf{(13)}$$

and

$$U_2 = \int_0^r \frac{N_1^2 d\rho}{2EA_1} \quad \textbf{(14)}$$

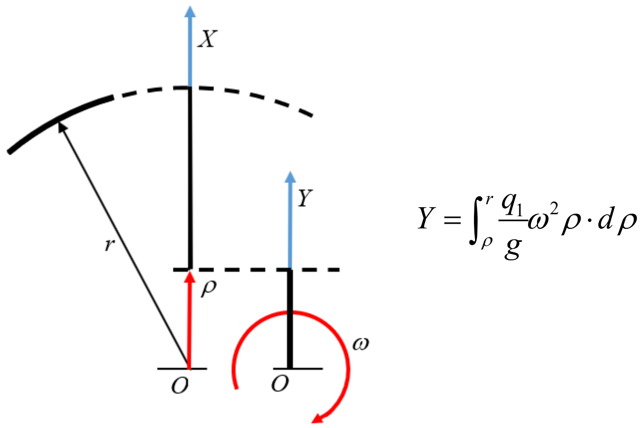

Figure 4. Calculation of normal effort in the rotating spoke.

The rotation in the section where M_0 acts is null. As for the internal force X , it ensures that the spoke does not separate from the ring (Pippard 1924), resulting, as shown in Annex 1:

$$\begin{cases} \frac{\partial}{\partial M_0}\left(U_1 + U_2\right) = 0 \\ \frac{\partial}{\partial X}\left(U_1 + U_2\right) = 0 \end{cases} \quad \textbf{(15)}$$

Figure 5 shows schematically the deformation, and is interpreted in Figure 6, (*e.g.*, Rötscher 1929), where ρ_K is the increase in the radius of the rotating rim if free from the action of the spokes, and λ_A is the increase in radius of the spoke if unconnected to the rim.

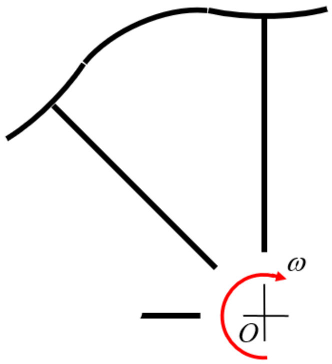

Figure 5. Schematical representation of the deformation of centerlines of rim and of spokes. Notice the expected changes of the bending moment sign between two spokes.

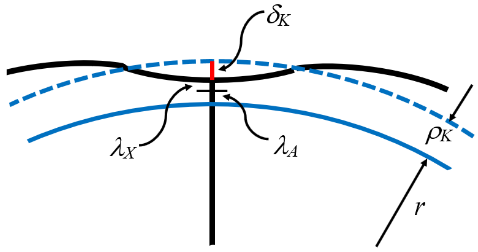

Figure 6. Schematical representation of the deformed centerline of rotating rim if unconnected to spokes (dashed arc of circle of radius $r+\rho_K$). λ_A : extension of rotating spokes if unconnected to rim.

As a result of the analysis detailed in Annex 1, M_0 and X are:

$$M_0=-\frac{Xr}{2}\left(\frac{1}{\sin\alpha}-\frac{1}{\alpha}\right) \tag{16}$$

$$X=\frac{2}{3}\frac{q\omega^2r^2}{g}\frac{1}{\frac{Ar^2}{I}f_2(\alpha)+f_1(\alpha)+\frac{A}{A_1}} \tag{17}$$

where

$$f_1(\alpha)=\frac{1}{2\sin^2\alpha}\left(\frac{\sin(2\alpha)}{4}+\frac{\alpha}{2}\right) \tag{18}$$

$$f_2(\alpha)=\frac{1}{2\sin^2\alpha}\left(\frac{\sin(2\alpha)}{4}+\frac{\alpha}{2}\right)-\frac{1}{2\alpha} \tag{19}$$

3. One detailed example

The analysis will be illustrated using data and expanding the presentation from (Timoshenko 1969): steel flywheel with 6 spokes rotating at 62.83 rad/s, radius of the centerline of the rim cross sections *r*=1500 mm, square cross section of the rim 300 mm × 300 mm, cross section area of each spoke assumed constant and equal to $A_1=15000\ \text{mm}^2$. Specific weight γ=7850 kgf/m^3 and *g*=9.8 m/s^2 are assumed. If the spokes do not limit the deformation of the ring (*i.e.*, the ring deforms freely),

$$\sigma_0 = \frac{\gamma}{g}(\omega r)^2 = 69.82 \text{ Nmm}^{-2}$$

If the spokes constrain the deformation of the ring, we can consider two cases: totally rigid spokes, or deformable spokes. The first situation is a limit case not occurring in practice but of interest for comparison.

Consider the limit case of the inextensible spokes. The problem is equivalent to that of a beam of length $l = \alpha r$ built-in at both ends, subject to a uniformly distributed load per unit of beam length:

$$\frac{q}{g}\omega^2 r = 4187 \text{ N/mm}=w$$

For this situation (Budynas and Nisbett 2011),

$$M = \frac{w}{12}\left(6\times l\times x - 6\times x^2 - l^2\right)$$

The evolution of the moment is represented in Figure 7, where φ is counted from a spoke.

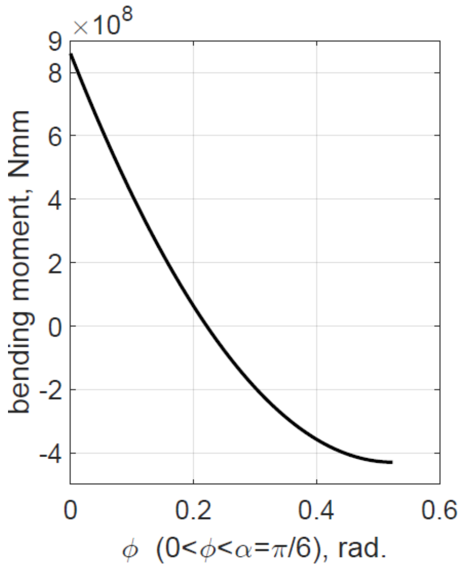

Figure 7. Bending moment *versus* φ. Inextensible spokes.

The evolution of the maximum and minimum stress along the arc is given in Figure 8.

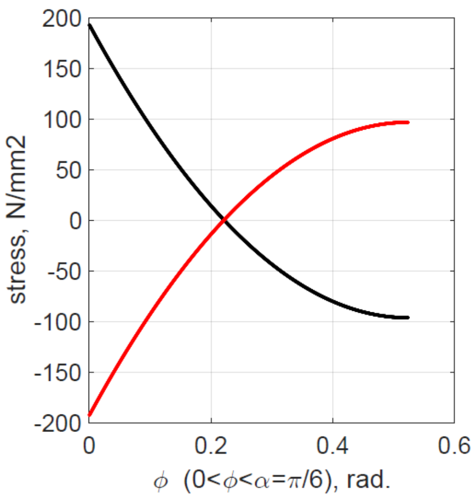

Figure 8. Stress in the ring *versus* φ, inextensible spokes. Black: inner fiber; red: outer fiber.

Figure 9 shows the evolution of the maximum positive values in each section. (Figure 9 consists of the positive part of the data in Figure 8).

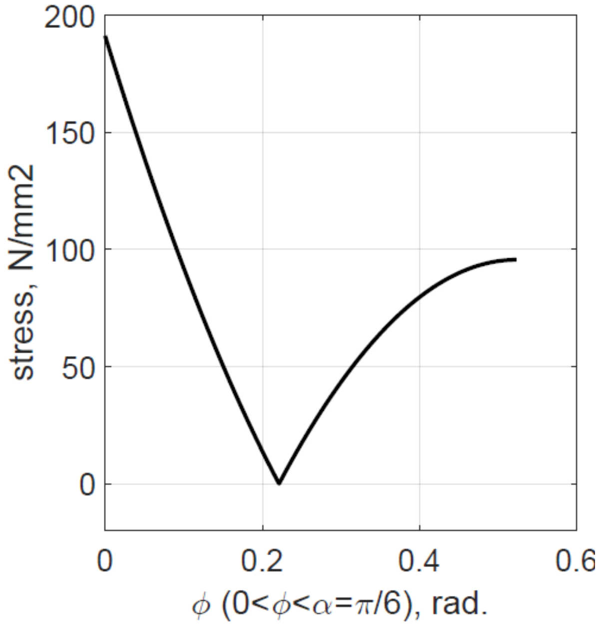

Figure 9. Rim stress *versus* φ , inextensible spokes.

Considering the deformation of the spokes, *i.e.,* the rigorous analysis recalled before, leads to the evolution of moment represented in Figure 10, and of maximum stress in Figure 11.

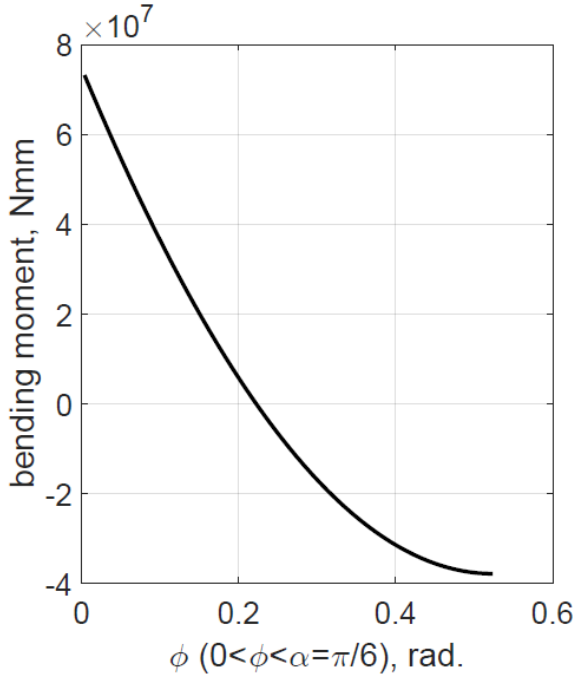

Figure 10. Bending moment *versus* φ . Deformable spokes.

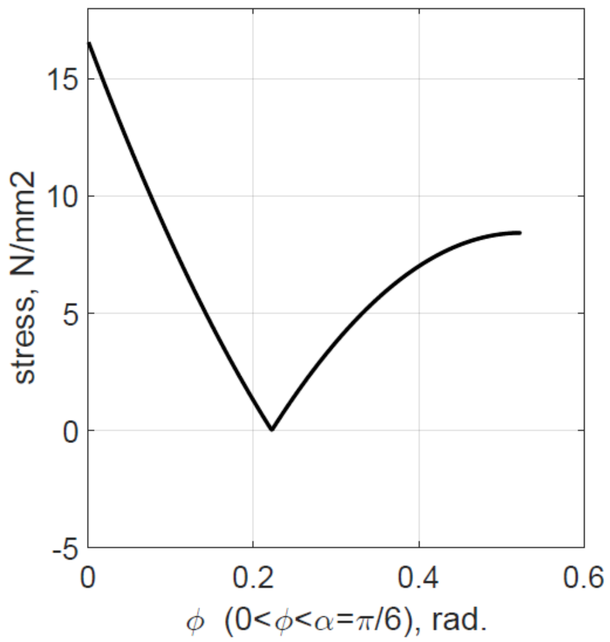

Figure 11. Rim stress, deformable spokes.

Now the total stress results from the bending effect (see above), and the normal effort (which did not exist in the extreme case of rigid spokes). Normal effort is

$$N = \frac{q}{g}\omega^2 r^2 - \frac{X\cos\varphi}{2\sin\alpha}$$

and in Figure 12 it appears to be almost constant, *i.e.*, approximately independent of φ (see dotted curve).

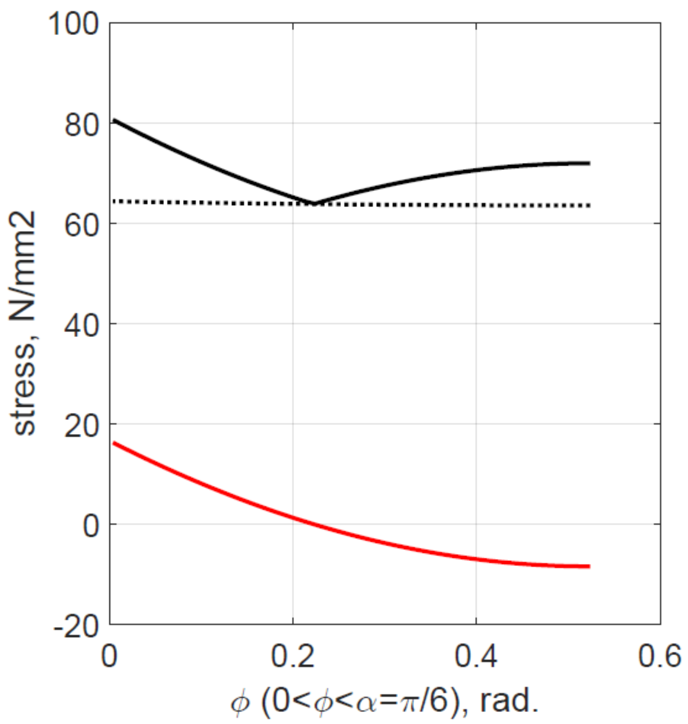

Figure 12. Stress as a function of bending moment (red); stress resulting from the normal effort (dotted line) and total resulting value (black full line).

The dependence of maximum stress on the number of spokes was examined for the same flywheel. Using the analytical solution recalled above, the maximum stress was calculated in the bisector between spokes, and in the ring cross section corresponding to a spoke, see Figure 13.

It is noted that there are other presentations of the subject. Hall *et al*. (Hall, Holowenko, and Laughlin 1961) give a so-called calculation formula, used for example in Akpobi *et al.* (Akpobi and Lawani 2006) and Wang *et al*. (Wang, Li, and Müller 2009). With manipulation presented in Annex 2, that calculation formula can be seen to be derived from the analysis just recalled.

The use of Lanza's approach, referred to above, would lead to the result:

$$\sigma = \left(\frac{3}{4}\right)\frac{\gamma}{g}(\omega r)^2 + \left(\frac{1}{4}\right)\frac{M_{\max} y_{\max}}{I} = 100.2 \text{ Nmm}^{-2}$$

which differs from the result of the full analysis, $\sigma_{\max} = 81.1 \text{ Nmm}^{-2}$, by 24%, on the safety side since it overestimates stress.

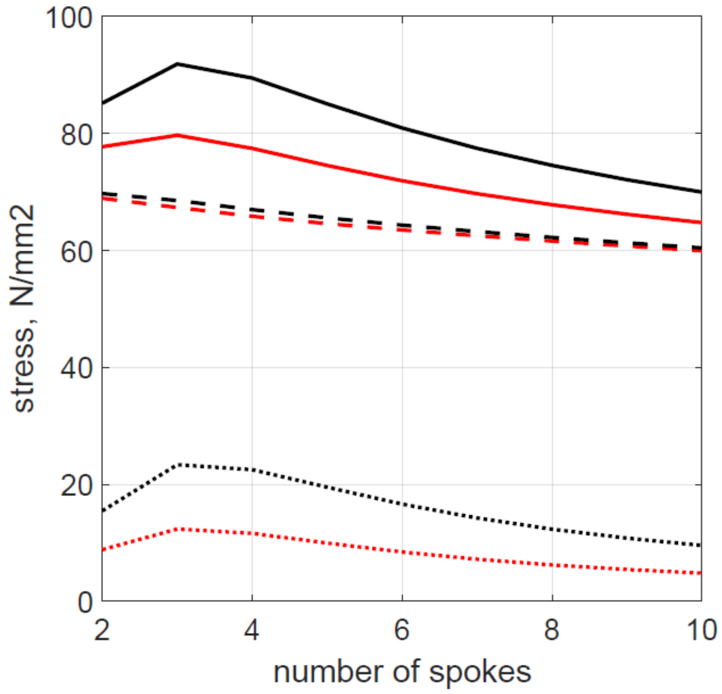

Figure 13 – Stress in the rim as a function of number of spokes. Spoke section – black; bisector section – red. Continuous lines: maximum total stress. Dashed lines: stress resulting from the normal effort. Dotted lines: stress resulting from the bending moment.

4. Bi-material flywheels. The effect of spokes' rigidity

The reference made to the approximate approach attributed to Lanza ('rule 3/4, 1/4', see above), raises the curiosity to examine in detail the influence of the stiffness of the spokes. The analytical solution recalled (see in particular equations 16 and 17 above), does not allow this analysis: it does not admit the possibility of different materials for ring and spokes, and in the equations the only reference to spokes is the ratio A/A_1 in the denominator of equation 17.

To address this issue, it is necessary to go back to an intermediate point in the analysis, described step by step in Annex 1, specifically its equation 25.

We will now admit that the spoke and ring materials have different Young's moduli, rewriting the terms that are related to the spokes. We get:

$$\frac{Xr^3}{EI}f_2-\frac{r^3q\omega^2}{EAg}+\frac{rX}{EA}f_1+\frac{Xr}{E_1A_1}+\frac{1}{3}\frac{q_1\omega^2r^3}{E_1A_1g}=0 \tag{20}$$

and then,

$$X=\frac{\frac{r^3q\omega^2}{EAg}-\frac{1}{3}\frac{q_1\omega^2r^3}{E_1A_1g}}{\frac{r^3}{EI}f_2+\frac{r}{EA}f_1+\frac{r}{E_1A_1}}=\frac{\frac{r^3q\omega^2}{Eg}-\frac{1}{3}\frac{q_1\omega^2r^3}{E_1g}\frac{A}{A_1}}{\frac{r^3A}{EI}f_2+\frac{r}{E}f_1+\frac{r}{E_1}\frac{A}{A_1}}=\frac{\frac{r^3q\omega^2}{g}-\frac{1}{3}\frac{q_1\omega^2r^3}{g}\frac{A}{A_1}\frac{E}{E_1}}{\frac{r^3A}{I}f_2+rf_1+r\frac{E}{E_1}\frac{A}{A_1}}$$

Considering that

$$q/A=\gamma \quad ; \quad q_1/A_1=\gamma_1 \quad ; \quad q_1=q\frac{A_1}{A}\frac{\gamma_1}{\gamma}$$

$$X=\frac{\frac{r^3q\omega^2}{g}-\frac{1}{3}\frac{q\omega^2r^3}{g}\frac{\gamma_1}{\gamma}\frac{E}{E_1}}{\frac{r^3A}{I}f_2+rf_1+r\frac{E}{E_1}\frac{A}{A_1}}=\frac{\frac{r^2q\omega^2}{g}-\frac{1}{3}\frac{q\omega^2r^2}{g}\frac{\gamma_1}{\gamma}\frac{E}{E_1}}{\frac{r^2A}{I}f_2+f_1+\frac{E}{E_1}\frac{A}{A_1}} \tag{21}$$

and recalling that E and γ are rim material properties, and E_1 and γ_1 correspond to the spokes, the equation 21 above is a general solution for the analytical stress analysis of a rotating rim and spokes bi-material flywheel.

For the sake of a parametric example, assume now an idealized situation where $\gamma/\gamma_1 = 1$ and E / E_1 may assume values between 0 and 1. In such an idealized situation,

$$\frac{q}{A}=\frac{q_1}{A_1}\rightarrow q_1=q\frac{A_1}{A}$$

and

$$X=\frac{\frac{r^2q\omega^2}{g}-\frac{1}{3}\frac{q\omega^2r^2}{g}\frac{E}{E_1}}{\frac{r^2A}{I}f_2+f_1+\frac{E}{E_1}\frac{A}{A_1}}$$

We may now examine the effect of spoke stiffness on the general stress distribution, just by varying the relationship E/E_1. Using the data from the example under consideration, Figure 14 illustrates the influence of the relationship E/E_1 on the bending moment value. The figure includes, for comparison, the case of the long straight beam of length $2r\alpha$, built-in at both ends, and loaded by the centrifugal force $(q/g)\omega^2r$ per unit length.

Given the assumptions of this example, obviously the curve for $E/E_1=1$ is equal to the curve presented in Figure 10, above.

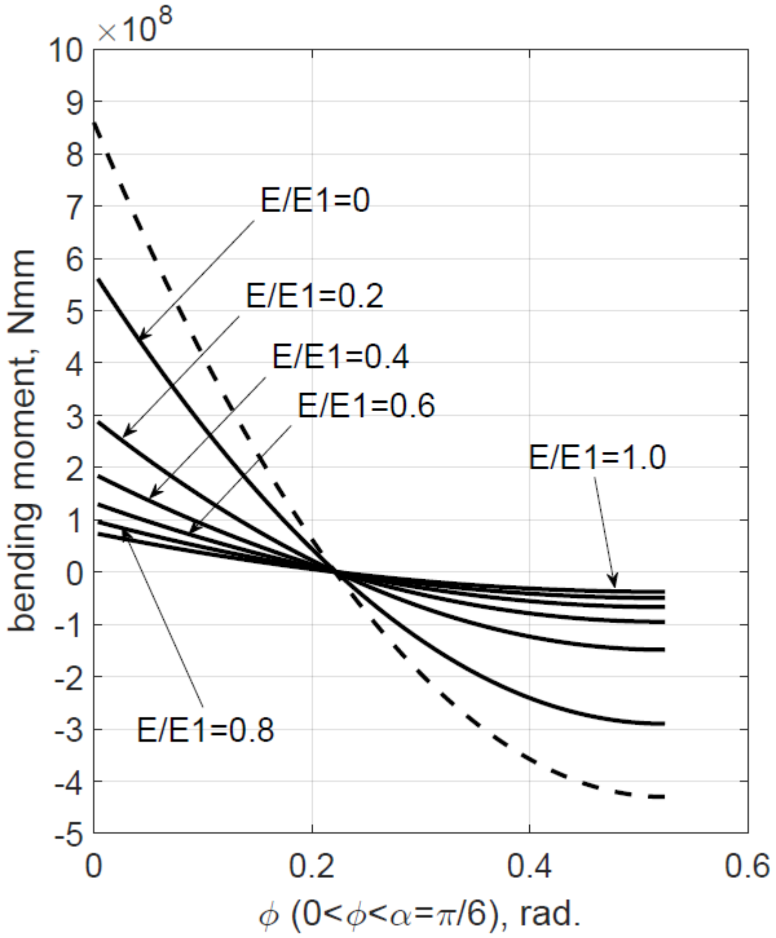

Figure 14. Influence of the ratio E/E_1 on the bending moment. Dashed line: case of the beam of length $l = 2r\alpha$. 6 spokes.

The solution for $E/E_1 = 0$ reflects the situation of rigid spokes, and is also shown in Figure 7. It presents a considerable difference in relation to the solution for the straight beam of length $2r\alpha$, built-in at both ends, and subjected to the load $(q/g)\omega^2 r$ per unit length. The difference between the dashed curve and the solution for $E/E_1 = 0$ should decrease with increasing number of spokes, *i.e.*, the approach based on a straight beam of length $2r\alpha$ should be better when α decreases.

Figure 15 repeats the analysis in Figure 14, but now for 10 spokes instead of 6. Clearly the rough simple solution considering each rim arc as a beam built in in its ends is now closer to the E/E_1 = 0 solution, a fact that is due to the greater similarity between the real case and the approximation - the curved arc is now closer to a straight line.

As expected, the difference between the situation of the rectilinear beam of length $2r\alpha$ built-in at both ends (dashed curve), and the solution for $E/E_1 = 0$ decreases with increasing number of spokes, *ie*, the approach based on a rectilinear beam is better when α decreases. Situations with more than 10 spokes, not included here, show that the agreement becomes even better.

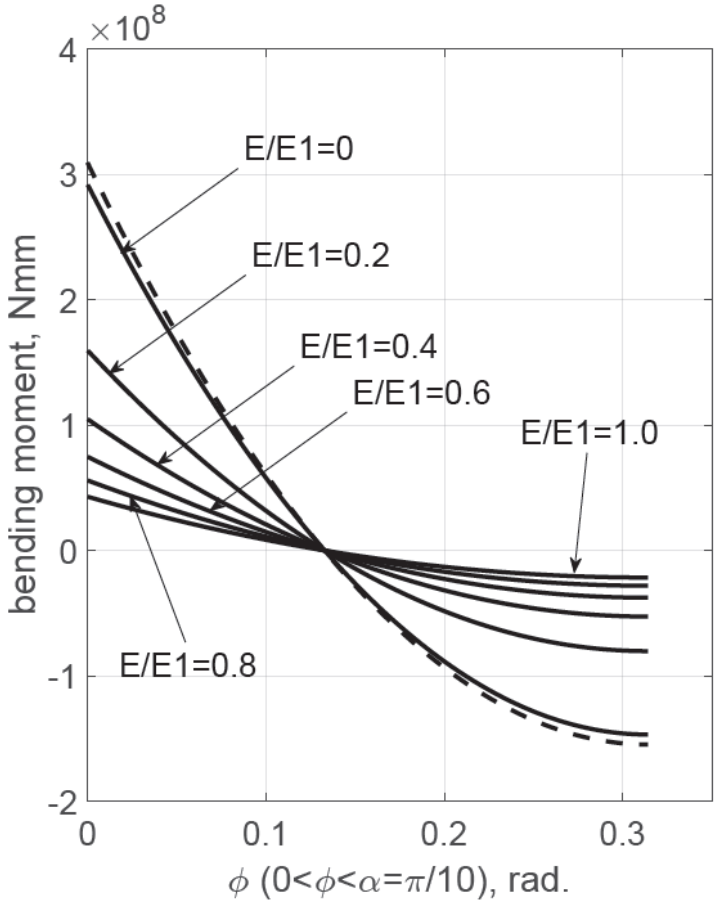

Figure 15. Influence of ratio E/E_1 on the bending moment. Dashed line: case of the beam of length $l = 2r\alpha$. 10 spokes.

Concluding remarks

- The past and outlook for the use of FESSs was concisely reviewed.
- The analytical stress analysis for a rotating rim and spokes flywheel based upon Castigliano's theorems was detailed.
- The analytical stress analysis for a bi-material flywheel is derived, and a parametric solution is presented.
- The origin of widely available design formulas is elucidated and their rational is discussed.

References

Akhil, Abbas A. et al. 2015 *DOE/EPRI Electricity Storage Handbook in Collaboration with NRECA*. Albuquerque, New Mexico, and Livermore, California: Sandia National Laboratories. https://doi.org/10.2172/1431469.

Akpobi, John A., and I. A. Lawani. 2006. "Computer-aided-design of flywheels". *Advances in Engineering Software* 37, no. 4: 222-235. https://doi.org/10.1016/j.advengsoft.2005.06.003.

AL Shaqsi, Ahmed Zayed, K. Sopian, and A. Al-Hinai. 2020. "Review of energy storage services, applications, limitations, and benefits". *Energy Reports* 6, suppl. 7: 288-306. https://doi.org/10.1016/j.egyr.2020.07.028.

Amiryar, Mustafa E., and K. R. Pullen. 2017. "A review of flywheel energy storage system technologies and their applications". *Applied Sciences* 7, no. 3: 286. https://doi.org/10.3390/app7030286.

Babuska, V., S. M. Beatty, B. J. deBlonk, and J. L. Fausz. 2004. "A review of technology developments in flywheel attitude control and energy transmission systems". 2004 IEEE Aerospace Conference Proceedings vol 4: 2784-2800. https://doi.org/10.1109/AERO.2004.1368076.

Beacon Power. 2018. "Carbon fiber flywheels". https://beaconpower.com/carbon-fiber-flywheels/.

Buchroithner, Amir. 2019. *Schwungradspeicher in der Fahrzeugtechnik*. Wiesbaden, Germany: Springer Viewveg. https://doi.org/10.1007/978-3-658-25571-8.

Buchroithner, Armin. 2018. "Effizienterer Einsatz von Schwungradspeichern in Fahrzeugen durch interdisziplinäre und multidimensionale Optimierung ihres Sub- und Supersystems". PhD Dissertation, Institut für Maschinenelemente und Entwicklungsmethodik, Technische Universität Graz. https://diglib.tugraz.at/effizienterer-einsatz-von-schwungradspeichern-in-fahrzeugen-durch-interdisziplinaere-und-multidimensionale-optimierung-ihres-sub-und-supersystems-2017.

Budynas, Richard. G., and J. K. Nisbett. 2011. *Shigley's Mechanical Engineering Design*. 9th ed. New York: McGraw-Hill. ISBN 978-0-07-352928-8.

Chen, Haisheng, T. N. Cong, W. Yang, C. Tan, Y. Li, and Y. Ding. 2009. "Progress in electrical energy storage system: A critical review". *Progress in Natural Science* 19, no. 3: 291-312. https://doi.org/10.1016/j.pnsc.2008.07.014.

Collins, Jack A., H. R. Busby, and G. H. Staab. 2010. *Mechanical Design of Machine Elements and Machines*. 2nd ed. Wiley. ISBN 978-0-470-41303-6.

Dahlberg, Tore. 2004. "Procedure to calculate deflections of curved beams". *International Journal of Engineering Education* 20, no. 3: 503-513. https://www.ijee.ie/articles/Vol20-3/IJEE1497.pdf.

Faires, Virgil M. 1980. *Elementos Orgânicos de Máquinas*. Rio de Janeiro: Livros Técnicos e Científicos Editora.

Genta, G. 1985. *Kinetic Energy Storage: Theory and Practice of Advanced Flywheel Systems*. Butterworth-Heinemann. ISBN 978-0-408-01396-3.

Hall, A. A., A. R. Holowenko, and H. G. Laughlin. 1961. *Schaum's Outline of Theory and Problems of Machine Design*. McGraw-Hill.

Hedlund, Magnus, J. Lundin, J. de-Santiago, J. Abrahamsson, and H. Bernhoff. 2015. "Flywheel energy storage for automotive applications". *Energies* 8, no. 10: 10636-10663. https://doi.org/10.3390/en81010636.

Ibrahim, H., A. Ilinca, and J. Perron. 2008. "Energy storage systems - Characteristics and comparisons". *Renewable and Sustainable Energy Reviews* 12, no. 5: 1221-1250. https://doi.org/10.1016/j.rser.2007.01.023.

Kardestuncer, H. 1978. "Castigliano's contribution to matrix structural analysis". *Computers & Structures* 9, no. 6: 547-549. https://doi.org/10.1016/0045-7949(78)90003-2.

Kent, W. 1895 "discussion of the article: G. Lanza, 'Stresses in the rims and rim-joints of pulleys and flywheels'". *Transactions of the ASME* XVI: 208-227.

Khurmi, R. S. and J. K. Gupta. 2005. *A Textbook of Machine Design*. New Delhi: Eurasia Publishing House (P.V.T.).

Kimball, Dexter S., and J. H. Barr. 1909. *Elements of Machine Design*. New York: Wiley.

Kitade, Shintarou. 2000 "Flywheel". In *Comprehensive Composite Materials* vol. 6: Design and Applications. A. Kelly and C. Zweben, eds. Elsevier. Pergamon. pp. 571-580. https://doi.org/10.1016/B0-08-042993-9/00123-6.

Lanza, G. 1895. "Stresses in the rims and rim-joints of pulleys and flywheels". *Transactions of the ASME* XVI: 208-227.

Lingaiah, K. 2004. *Machine Design Databook*. McGraw-Hill.

Liu, Haichang and J. Jiang. 2007 "Flywheel energy storage - An upswing technology for energy sustainability". *Energy and Buildings* 39, no. 5: 599–604. https://doi.org/10.1016/j.enbuild.2006.10.001.

Longbottom, J. G. 1924. "Communication on A. J. S. Pippard, 'The stresses in a uniformly rotating fly-wheel'". *Proceedings of the Institution of Mechanical Engineers* 106, no. 1: 22-51 (see 43-51).

Luo, Xing, J. Wang, M. Dooner, and J. Clarke. 2015. "Overview of current development in electrical energy storage technologies and the application potential in power system operation". *Applied Energy* 137: 511-536. https://doi.org/10.1016/j.apenergy.2014.09.081.

Mata, Antonio Simón et al. 2016. *Fundamentals of Machine Theory and Mechanisms*. Springer. https://doi.org/10.1007/978-3-319-31970-4.

Pärnamäe, Ragne et al. 2020. "The acid–base flow battery: sustainable energy storage via reversible water dissociation with bipolar membranes". *Membranes* 10, no. 12. https://doi.org/10.3390/membranes10120409.

Pippard, A. J. S. 1924. "The stresses in a uniformly rotating fly-wheel". *Proceedings of the Institution of Mechanical Engineers* 106, no. 1: 25-51.

Pullen, Keith Robert, ed. Energies. 2021. "Flywheel Energy Storage Systems and Applications". Special Issue of *Energies. D: Energy Storage and Application*. https://www.mdpi.com/journal/energies/special_issues/FESS.

PUNCH Flybrid. 2022. PUNCH Flybrid. https://punchflybrid.com/.

RICARDO PLC. 2011. "Breakthrough in Ricardo Kinergy 'second generation' high-speed flywheel technology". https://ricardo.com/news-and-media/news-and-press/breakthrough-in-ricardo-kinergy-%E2%80%98second-generation.

Richma, R. H. 1997. *Flywheel Energy Storage*. EPRI TR-108378. Palo Alto, California: EPRI. https://www.epri.com/research/products/TR-108378.

Rötscher, Felix. 1929. *Die Maschinenelemente*. Berlin: Springer. ISBN 978-3-662-37225-8.

The Economist. 2011. "Reinventing the wheel". *The Economist: Technology Quarterly: Flywheels*, 3rd December. https://www.economist.com/technology-quarterly/2011/12/03/reinventing-the-wheel.

Timoshenko, Stephen P. 1969. *Resistência dos Materiais*. Rio de Janeiro: Ao Livro Técnico.

Vullo, Vincenzo and F. Vivio. 2013. *Rotors: Stress Analysis and Design*. Springer-Verlag Italia. https://doi.org/10.1007/978-88-470-2562-2.

Wang, Jifeng, Q. Li, and N. Müller. 2009. "Mechanical and optimization analyses for novel wound composite axial impeller". *Proceedings of the ASME 2009 International Mechanical Engineering Congress and Exposition. Volume 11: Mechanics of Solids, Structures and Fluids*. Lake Buena Vista, Florida, USA. November 13-19. pp. 49-53. https://doi.org/10.1115/IMECE2009-12938.

Acknowledgments

Remarks of Rui Martim Salgado and João Duarte Marafona on initial versions of this manuscript are gratefully acknowledged.

Annex 1

This annex presents the calculation based on Castigliano's theorem, whose final result is presented in (Timoshenko 1969). Beginning by

$$\frac{\partial}{\partial M_0}\left(U_1+U_2\right)=0$$

and, as previously discussed,

$$U_1=2\int_0^{\alpha}\frac{M^2rd\varphi}{2EI}+2\int_0^{\alpha}\frac{N^2rd\varphi}{2EA}\quad ;\quad U_2=\int_0^{r}\frac{N_1^2d\rho}{2EA_1}$$

Since U_2 and N do not depend upon M_0, we get

$$\frac{\partial}{\partial M_0}\left(U_1+U_2\right)=0\rightarrow\frac{\partial}{\partial M_0}\left(2\int_0^{\alpha}\frac{M^2rd\varphi}{2EI}\right)=0$$

Being

$$M=M_0+\frac{Xr}{\sin\alpha}\sin^2\left(\frac{\varphi}{2}\right)\rightarrow\frac{\partial M}{\partial M_0}=1$$

Therefore,

$$\frac{\partial}{\partial M_0}\left(2\int_0^{\alpha}\frac{M^2rd\varphi}{2EI}\right)=0=\frac{2}{EI}\int_0^{\alpha}M\frac{\partial M}{\partial M_0}rd\varphi=\frac{2r}{EI}\int_0^{\alpha}M\frac{\partial M}{\partial M_0}d\varphi=$$

$$\frac{2r}{EI}\int_0^{\alpha}\left[M_0+\frac{Xr}{\sin\alpha}\sin^2\left(\frac{\varphi}{2}\right)\right]d\varphi=\frac{2r}{EI}M_0\alpha+\frac{2r}{EI}\left(\frac{Xr\alpha}{2\sin\alpha}-\frac{Xr}{2}\right)=0$$

$$\therefore M_0=-\frac{Xr}{2}\left(\frac{1}{\sin\alpha}-\frac{1}{\alpha}\right)$$

The other equation requires much greater attention and time. Being

$$\frac{\partial}{\partial X}\left(U_1+U_2\right)=0$$

Recall that

$$M=M_0+\frac{Xr}{\sin\alpha}\sin^2\left(\frac{\varphi}{2}\right)=-\frac{Xr}{2}\left(\frac{1}{\sin\alpha}-\frac{1}{\alpha}\right)+\frac{Xr}{\sin\alpha}\sin^2\left(\frac{\varphi}{2}\right)$$

$$N=\frac{q\omega^2r^2}{g}-\frac{X\cos\varphi}{2\sin\alpha}$$

$$N_1=X+\frac{q_1\omega^2}{2g}\left(r^2-\rho^2\right)$$

Resulting

$$\frac{\partial M}{\partial X}=-\frac{r}{2}\left(\frac{1}{\sin\alpha}-\frac{1}{\alpha}\right)+\frac{r}{\sin\alpha}\sin^2\frac{\varphi}{2}$$

$$\frac{\partial N}{\partial X}=-\frac{\cos\varphi}{2\sin\alpha}$$

$$\frac{\partial N_1}{\partial X}=-1$$

Let us calculate

$$\frac{\partial}{\partial X}\left(U_1+U_2\right)=0$$

being

$$U_1=2\int_0^{\alpha}\frac{M^2rd\varphi}{2EI}+2\int_0^{\alpha}\frac{N^2rd\varphi}{2EA}\quad ;\quad U_2=\int_0^{r}\frac{N_1^2d\rho}{2EA_1}$$

$$\frac{\partial}{\partial X}\left(U_1+U_2\right)=\frac{2}{EI}\int_0^{\alpha}M\frac{\partial M}{\partial X}rd\varphi+\frac{2}{EA}\int_0^{\alpha}N\frac{\partial N}{\partial X}rd\varphi+\frac{1}{EA_1}\int_0^{\alpha}N_1\frac{\partial N_1}{\partial X}d\rho=0$$

First integral:

$$\frac{2}{EI}\int_0^{\alpha}M\frac{\partial M}{\partial X}rd\varphi=$$

$$=\frac{2r}{EI}\int_0^{\alpha}\left(-\frac{Xr}{2}\left(\frac{1}{\sin\alpha}-\frac{1}{\alpha}\right)+\frac{Xr}{\sin\alpha}\sin^2\left(\frac{\varphi}{2}\right)\right)\left(-\frac{r}{2}\left(\frac{1}{\sin\alpha}-\frac{1}{\alpha}\right)+\frac{r}{\sin\alpha}\sin^2\frac{\varphi}{2}\right)rd\varphi=$$

Using the transformation

$$\sin^2\frac{\varphi}{2}=\frac{1-\cos\varphi}{2}$$

$$\frac{2}{EI}\int_0^{\alpha}M\frac{\partial M}{\partial X}rd\varphi=\frac{2r}{EI}\int_0^{\alpha}\left(\frac{r}{\alpha}-\frac{r}{\sin\alpha}\frac{\cos\varphi}{2}\right)\cdot\frac{X}{4}\left(\frac{r}{\alpha}-\frac{r}{\sin\alpha}\frac{\cos\varphi}{2}\right)d\varphi=$$

$$=\frac{Xr^3}{2EI}\int_0^{\alpha}\left(\frac{1}{\alpha^2}-\frac{2\cos\alpha}{\alpha\sin\alpha}+\frac{\cos^2\varphi}{\sin^{2\varphi}}\right)d\varphi=-\frac{Xr^3}{2EI\alpha}+\frac{Xr^3}{2EI}\left[\frac{1}{\sin^2\alpha}\left(\frac{\alpha}{2}+\frac{\sin 2\alpha}{4}\right)\right]$$

And defining

$$f_2=\frac{1}{2\sin^2\alpha}\left(\frac{\alpha}{2}+\frac{\sin 2\alpha}{4}\right)-\frac{1}{2\alpha}$$

$$\frac{2}{EI}\int_0^{\alpha}M\frac{\partial M}{\partial X}rd\varphi=\frac{Xr^3}{EI}f_2 \qquad (\mathbf{22})$$

Second integral:

$$\frac{2}{EA}\int_0^{\alpha}N\frac{\partial N}{\partial X}rd\varphi=\frac{2}{EA}\int_0^{\alpha}\left(\frac{q\omega^2r^2}{g}-\frac{X\cos\varphi}{2\sin\alpha}\right)\left(-\frac{\cos\varphi}{2\sin\alpha}\right)rd\varphi=$$

$$=\frac{2}{EA}\int_0^{\alpha}\left(-\frac{q\omega^2r^2}{g}\frac{\cos\varphi}{2\sin\alpha}+\frac{X\cos^2\varphi}{4\sin^2\alpha}\right)d\varphi=-\frac{r^3q\omega^2}{EAg}+\frac{rX}{EA2\sin^2\alpha}\left(\frac{\alpha}{2}+\frac{\sin 2\alpha}{4}\right)$$

Let it be

$$f_1=\frac{1}{2\sin^2\alpha}\left(\frac{\alpha}{2}+\frac{\sin 2\alpha}{4}\right)$$

resulting

$$\frac{2}{EA}\int_0^{\alpha} N\frac{\partial N}{\partial X}rd\varphi = -\frac{r^3 q\omega^2}{EAg} + \frac{rX}{EA}f_1 \tag{23}$$

Finally, third integral,

$$\frac{1}{EA_1}\int_0^{\alpha} N_1\frac{\partial N_1}{\partial X}d\rho = \frac{1}{EA_1}\int_0^{\alpha}\left(X + \frac{q_1\omega^2}{2g}\left(r^2-\rho^2\right)\right)d\rho = \frac{Xr}{EA_1} + \frac{1}{3}\frac{q_1\omega^2 r^3}{EA_1 g} \tag{24}$$

Adding (20), (21), e (22), and equating to zero

$$\begin{aligned}
&\frac{Xr^3}{EI}f_2 - \frac{r^3 q\omega^2}{EAg} + \frac{rX}{EA}f_1 + \frac{Xr}{EA_1} + \frac{1}{3}\frac{q_1\omega^2 r^3}{EA_1 g} = 0\\
&\frac{Xr^3}{EI}f_2 - \frac{r^3 q\omega^2}{EAg} + \frac{rX}{EA}f_1 + \frac{Xr}{EA_1} + \frac{1}{3}\frac{q_1\omega^2 r^3}{EA_1 g} =\\
&\rightarrow X\left(\frac{r^3}{I}f_2 + \frac{r}{A}f_1 + \frac{r}{A_1}\right) = \frac{r^3 q\omega^2}{Ag} - \frac{1}{3}\frac{q_1\omega^2 r^3}{A_1 g}
\end{aligned} \tag{25}$$

Dividing by r

$$X\left(\frac{r^2}{I}f_2 + \frac{1}{A}f_1 + \frac{1}{A_1}\right) = \frac{r^2 q\omega^2}{Ag} - \frac{1}{3}\frac{q_1\omega^2 r^2}{A_1 g}$$

And multiplying by A

$$X\left(\frac{r^2 A}{I}f_2 + f_1 + \frac{A}{A_1}\right) = \frac{r^2 q\omega^2}{g} - \frac{1}{3}\frac{Aq_1\omega^2 r^2}{A_1 g}$$

Recalling that, with γ as specific weight common to rim and spokes, we have,

$$\begin{cases}\gamma A = q\\ \gamma A_1 = q_1\end{cases}$$

i.e.,

$$\frac{q_1}{A_1} = \frac{q}{A}$$

finally, we get

$$X\left(\frac{r^2 A}{I}f_2 + f_1 + \frac{A}{A_1}\right) = \frac{r^2 q\omega^2}{g} - \frac{1}{3}\frac{q\omega^2 r^2}{g} = \frac{2}{3}\frac{r^2 q\omega^2}{g}$$

And the result (given in (Timoshenko 1969) in a single line)

$$X = \frac{2}{3}\frac{r^2 q\omega^2}{g}\frac{1}{\dfrac{r^2 A}{I}f_2 + f_1 + \dfrac{A}{A_1}} \tag{26}$$

Annex 2

Starting from the solution presented in (Timoshenko 1969) with b,t as the length of the sides of the rim cross section.

$$\sigma=\frac{N}{b\times t}\pm\frac{M\times\frac{t}{2}}{\frac{bt^3}{12}}=\frac{\frac{q\omega^2r^2}{g}-\frac{X\cos\varphi}{2\sin\alpha}}{bt}\pm\frac{\left[M_0+\frac{Xr}{\sin\alpha}\sin^2\left(\frac{\varphi}{2}\right)\right]\times\frac{t}{2}}{\frac{bt^3}{12}}$$

$$M_0=-\frac{Xr}{2}\left(\frac{1}{\sin\alpha}-\frac{1}{\alpha}\right)$$

$$\sigma=\frac{q\omega^2r^2}{btg}-\frac{X\cos\varphi}{bt2\sin\alpha}\pm\frac{6}{bt^2}\left[-\frac{Xr}{2}\left(\frac{1}{\sin\alpha}-\frac{1}{\alpha}\right)+\frac{Xr}{\sin\alpha}\sin^2\left(\frac{\varphi}{2}\right)\right]$$

$$\sigma=\frac{q\omega^2r^2}{btg}-\frac{X}{bt}\left\{\frac{\cos\varphi}{2\sin\alpha}\pm\frac{6}{t}\left[\frac{r}{\sin\alpha}\sin^2\left(\frac{\varphi}{2}\right)-\frac{r}{2}\left(\frac{1}{\sin\alpha}-\frac{1}{\alpha}\right)\right]\right\}$$

$$\sigma=\frac{q\omega^2r^2}{btg}-\frac{X}{bt}\left[\frac{\cos\varphi}{2\sin\alpha}\pm\left(\frac{6r}{t\sin\alpha}\sin^2\left(\frac{\varphi}{2}\right)-\frac{3r}{t\sin\alpha}+\frac{3}{t\alpha}\right)\right]$$

Recalling that

$$X=\frac{2}{3}\frac{q\omega^2r^2}{g}\frac{1}{\frac{Ar^2}{I}f_2(\alpha)+f_1(\alpha)+\frac{A}{A_1}}$$

$$f_1(\alpha)=\frac{1}{2\sin^2\alpha}\left(\frac{\sin(2\alpha)}{4}+\frac{\alpha}{2}\right)$$

$$f_2(\alpha)=\frac{1}{2\sin^2\alpha}\left(\frac{\sin(2\alpha)}{4}+\frac{\alpha}{2}\right)-\frac{1}{2\alpha}$$

We get

$$\sigma=\frac{q\omega^2r^2}{btg}-\frac{2q\omega^2r^2}{3btg}\frac{1}{\frac{Ar^2}{I}f_2+f_1+\frac{A}{A_1}}\times[.......]$$

$$\sigma=\frac{q\omega^2r^2}{btg}\times\left[1-\frac{2}{3}\frac{\frac{\cos\varphi}{2\sin\alpha}\pm\left(\frac{3r}{t\sin\alpha}\left(2\sin^2\left(\frac{\varphi}{2}\right)-1\right)+\frac{3}{t\alpha}\right)}{\frac{btr^2}{\frac{bt^3}{12}}f_2+f_1+\frac{A}{A_1}}\right]$$

But

$$\sin^2\left(\frac{\varphi}{2}\right)=\frac{1-\cos\varphi}{2}$$

Doing

$$\frac{btr^2}{\frac{bt^3}{12}} f_2 + f_1 + \frac{A}{A_1} = 12\frac{r^2}{t^2} f_2 + f_1 + \frac{A}{A_1} = C$$

we get

$$\sigma = \frac{q\omega^2 r^2}{btg} \times \left[1 - \frac{\frac{\cos\varphi}{\sin\alpha} \pm \left(\frac{3r2}{t\sin\alpha} \times \left(-\cos\varphi\right) + \frac{3\times 2}{2t\alpha} \right)}{3C} \right]$$

$$\sigma = \frac{q\omega^2 r^2}{btg} \times \left[1 - \frac{\cos\varphi}{3C\sin\alpha} \pm \frac{r2}{tC}\left(\frac{1}{\alpha} - \frac{\cos\varphi}{\sin\alpha} \right) \right] \quad \textbf{(27)}$$

which is the expression given in (Hall, Holowenko, and Laughlin 1961), (Akpobi and Lawani 2006), and (Wang, Li, and Müller 2009).